Perception of a Haptic Jamming Display: Just Noticeable Differences in Stiffness and Geometry

Adam M. Genecov agenecov@stanford.edu
Andrew A. Stanley astan@stanford.edu
Allison M. Okamura aokamura@stanford.edu

Department of Mechanical Engineering, Stanford University

Abstract

This work characterizes aspects of human perception of a Haptic Jamming device, a tactile display capable of simultaneously and independently controlling its stiffness and geometry via particle jamming and pneumatic actuation. A single Haptic Jamming cell is filled with coarse coffee grounds, connected to vacuum, and placed over a pressure-regulated air chamber. Increased vacuum level in the cell increases cell stiffness, and increased pressure in the chamber beneath the cell balloons the cell upward. Single-cell devices were manufactured and tested to determine the relationships between the vacuum and air pressure levels and the device outputs, stiffness and geometry, respectively. Using these relationships, reference and comparison values were selected for each output, and psychophysical experiments were conducted to determine the Weber Fraction for rigidity (an alternate terminology for nonlinear stiffness, used in the experiment prompt) and geometry, represented by the eccentricity of the elliptical profile of the cell. The Weber Fractions for stiffness and geometry were 16.0% and 14.3%, respectively. No significant correlation was found between human perception of these stimuli and the forces/torques applied to the devices during haptic exploration. These results will enable more accurate representations of virtual environments using an array of haptic jamming cells under development for medical training and simulation.

Index Terms: H.5.2 [Information Interfaces and Presentation]: User Interfaces—Haptic I/O; H.1.2 [Models and Principles]: User/Machine Systems—Human factors; L.2.0.b [Haptics]: Haptics Technology—Tactile Devices;

1 Introduction

An "encountered-type" tactile display allows a user to freely explore a virtual environment. Ideally, the display does not require the user to wear or hold the device and can present new or changing information about the environment whenever the user touches it. This type of device has been previously developed with many different technologies. Pin arrays have been used to convey force and shape information to the fingertip, e.g. [1]. Rheological fluids arrays can change their mechanical properties when subjected to either electric [2] or magnetic [3] fields. "Digital clay" has been proposed as a controllably deformable surface for both computer input and output; one device uses an array of fluidic-driven actuators [4].

Most tactile displays specialize in controlling either geometry or stiffness, but not both. This paper expands on the previous development of a novel haptic surface display that can control both its stiffness and its geometry [5]. Briefly, this Haptic Jamming device uses an array of hollow silicone cells filled with coarse coffee grounds; each cell is capable of changing its stiffness by vacuuming the inside of the cell, thereby jamming the particles of the coffee grounds together and presenting an overall more rigid substance. The array is clamped over a pressure-regulated air chamber. In a cell's soft state, increasing the air pressure to inflate the chamber underneath results in the cell ballooning outward. By selectively vacuuming cells in an array and adjusting the chamber pressure, different material stiffnesses and geometries can be presented (Figure 1).

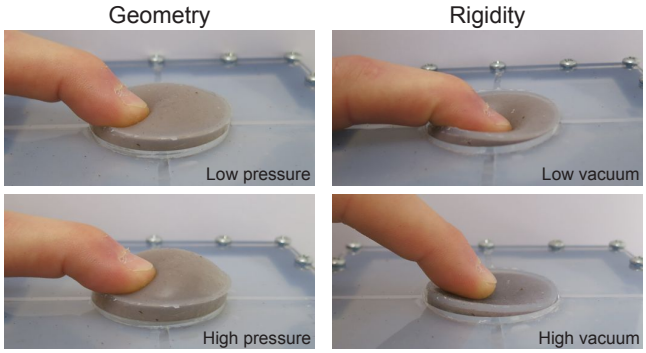

Figure 1: Single haptic jamming cells displaying different possible outputs. (Top left) A cell at low chamber pressure and no vacuum, producing a slightly ellipsoidal lump. (Bottom left) A cell at high chamber pressure and no vacuum, producing a less eccentric ellipsoid. (Top right) A cell at no vacuum and no chamber pressure, producing a highly compliant lump. (Bottom right) A cell at high vacuum and no chamber pressure, producing a flatter and highly rigid lump.

Previous experiments with single-cell versions of the device have characterized the effects of cell diameter, air pressure, vacuum level, and support type on the geometry and compliance of the cell [5]. This paper adds to the previous empirical characterization of device output by measuring user perception of changes in geometry and stiffness, defined by the just noticeable difference (JND), point of subjective equality (PSE), and corresponding Weber Fractions (WF). We first review the technology behind Haptic Jamming and previous research on user perception of geometry and compliance; we then describe our experimental procedures and report the calculated JNDs, PSEs, and WFs. The device was originally designed for an encountered-type combined cutaneous/kinesthetic display for medical training; characterization of user perception will allow for more accurate and useful presentation of virtual medical environments to users.

2 Background

The concept of particle jamming has been heavily researched by physicists and materials scientists for decades, and has recently spurred numerous applications in engineering fields. Several robotics applications use the ability to rapidly change a material's properties back and forth between flexible and rigid states, including a universal gripper that can deform around an object before becoming rigid to pick it up [11], a flexible cable-driven manipulator that can become rigid in any configuration [12], and a shell of particle jamming cells that enable robotic locomotion of a ball-like

structure [13]. The ability to deform and stiffen a material has also inspired a number of novel tactile user interfaces [14] [15] [16]. Moving beyond simply switching between flexible and rigid states to adjusting the levels in between, Mitsuda et al. [17] developed a particle jamming tube that runs along the length a user's arm to simulate moving through virtual environments of varying viscosity and stiffness.

This study is also related to a vast literature on stiffness and geometry perception. An elastic object's *stiffness* describes its resistance to deformation when a force is applied. The mechanical behavior of the particle jamming cells used in our work cannot be characterized as a pure stiffness, as the resistance also depends on deformation rate, In addition, the cells are not completely elastic (plastic deformation is possible) and the stiffness is nonlinear (although it is nearly linear for a range of applied force). Yet, we consider stiffness (or rigidity) to be the most succinct description of the dominant mechanical property of a particle jamming cell. The perceived stiffness of a particle jamming cell is likely due to the force-displacement relationship resulting from a combination of (1) the deformation of the surface of the cell and (2) gross movement of the cell in the direction of the applied force. Many studies exist that quantify human stiffness discrimination capabilities (e.g. [8, 9, 10]), and stiffness WFs have been reported ranging from 0.15 to 0.99. In our study, subjects freely explore a physical surface with a single hand in order to determine the size of a particle jamming cell. Thus, stereognosis (which invokes both tactile and proprioceptive modalities) is used to identify cell size. While there is a growing literature on size perception of stimuli such as ours for moving single point contacts, as well as multiple static point contacts, we have found no existing WF measurements for size perception during free surface exploration.

3 Methods

We built two single-cell Haptic Jamming devices and determined mathematical best-fit relationships between actuation levels (cell vacuum and chamber pressure) and the corresponding device output properties (stiffness and size, respectively). We then used the devices in a two-alternative forced choice psychophysical experiment in order to characterize human perception of these device properties.

3.1 Device Design and Control

Following the manufacturing procedures described in detail in [5], we constructed two 1.5-inch diameter circular-cell haptic jamming devices. These devices were constructed with the cell in the unsupported configuration, meaning that there was no physical support directly beneath the cell itself. Rather, it was suspended from the edges by a layer of silicone clamped between the acrylic pieces outside the cell. The boxes were assembled from laser-cut acrylic, and the silicone cells were created from custom laser-cut acrylic molds. The silicone cells had a 1/16-inch wall thickness and a 0.414-cubic-inch volume; each was filled with 7 teaspoons of coarse coffee grounds, slightly more than the nominal volume of the cell in order to prevent sagging over the unsupported air chamber.

As shown in Figure 2, the air chamber of each device was connected to a QB3TFEE003-S17 electronic pressure regulator (Proportion Air, McCordsville, Indiana), which in turn was connected to a 15 psi air pressure supply. Each pressure regulator outputs 0-3 psi, corresponding linearly to a 0-5 V command signal. The coffee-ground-filled cell of each device was connected first to a A04-BW1 three-way solenoid valve (Mead Fluid Dynamics, Inc., Chicago, IL) that exhausted to atmospheric pressure. The valve was then connected to an electronic vacuum regulator (Proportion Air, McCordsville, Indiana), which in turn was connected to a 26 inHg vacuum supply. Each vacuum regulator outputs 0-25 inHg of negative pressure, corresponding linearly to a 0-5 V command signal. All valves and regulators were controlled by computer using an National Instruments USB X Series DAQ interface.

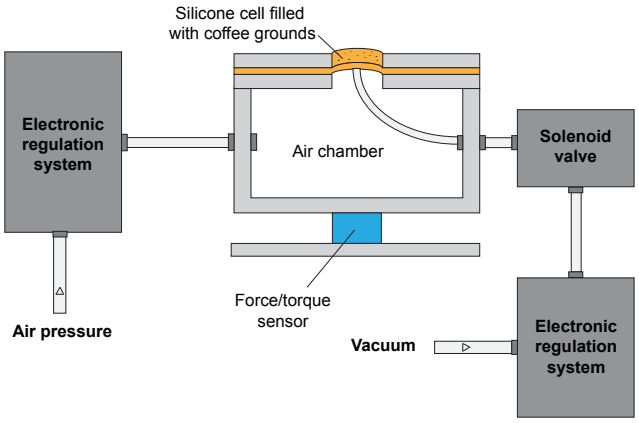

Figure 2: Schematic showing the pneumatic actuators and electronic regulators connected to a single device. The air chamber was connected to wall air pressure, and the inside of the coffee-ground-filled cell was connected to wall vacuum. Both air pressure and vacuum level were independently controlled by computer. A three-way solenoid valve was connected downstream of the vacuum regulator to allow for quick switching between vacuum and atmospheric pressure.

3.2 Relationship between Pneumatic Actuation and Device Properties

In order to accurately present rigidity (an alternate terminology for nonlinear stiffness, used in the experiment prompt) and geometry/size stimuli to our subjects, we characterized (1) the relationship between vacuum level and stiffness, and (2) the relationship between chamber pressure and size.

No stiffness data had previously been collected on an unsupported cell, so we obtained force-deflection curves at varying vacuum levels for both experimental devices. Similar to [5], we attached an ATI Nano17 force/torque sensor (ATI, Apex, NC) to a 9.5 mm 3D-printed plastic hemisphere. This assembly was attached to the end effector of a SensAble Phantom Premium 1.5 (SensAble Technologies, Inc., Wilmington, MA) robot, which was manually pushed down on the cell (Figure 3). The end effector was positioned directly above the center of the cell and was constrained to move only along the vertical axis. The Phantom also collected position data along this axis as the end effector depressed the surface of the cell. A baseline chamber pressure of 0.6 psi was maintained in order to restore cell shape after every trial. Each trial was performed on both devices for eleven vacuum levels and for five times for each vacuum level.

We calculated an overall stiffness for each trial by finding the force applied at 5 mm of deflection, where the force-deflection curve was still approximately linear in all trials. The stiffness was computed from this linear region; an average stiffness at each vacuum level was obtained from all corresponding trials. Average stiffness was plotted against vacuum level and fit to a power function using a least-squares cost function. The model used was of the form

$$K = \alpha_1 + \beta_1 v^{\gamma_1}, \tag{1}$$

where K is the stiffness in N/m, v is the vacuum level in in Hg, and α_1, β_1, and γ_1 are the fit parameters. This form of model was chosen based on a visual assessment of the plot and knowing that even at no vacuum (i.e. 0 in Hg), the cell has some baseline stiffness, necessitating the α_1 parameter. The results of this experiment are presented in Section 4.1 and were used to select comparison and reference values for the stiffness psychophysical experiment.

Figure 3: Setup used to measure force-deflection data for a single haptic jamming cell. A force/torque sensor was attached to the end effector of a Phantom Premium robot and was used to manually palpate the center of the cell. Position data was recorded from the Phantom Premium.

We used data collected in [5] to quantify how chamber pressure affects geometry. In that prior work, the geometry data was reported as the eccentricity a/b of the elliptical profile of the inflated cell (where a is the semi-major axis and b is the semi-minor axis). However, this metric yields an infinite eccentricity for an uninflated cell (when chamber pressure is 0 psi). We therefore inverted the data and plotted pressure against 1/Eccentricity b/a in order to form a plot similar to that obtained when evaluating stiffness, and the data was fit to a power function using a least-squares cost function. The model used was of the form

$$s = \alpha_2 p^{\beta_2}, \tag{2}$$

where s is 1/Eccentricity, p is the chamber pressure in psi, and α_2 and β_2 are the fit parameters. This model type was chosen based on a visual assessment of the plot and knowing that at no pressure (i.e. 0 psi), the cell is flat and has a 1/Eccentricity of 0. The results of this experiment are presented in Section 4.1 and were used to select comparison and reference values for the geometry psychophysical experiment.

3.3 Psychophysical Experiments

3.3.1 Subjects

Nine healthy subjects were used to measure the JND, PSE, and WF of stiffness and geometry for the Haptic Jamming devices. The subjects consisted of eight males and one female; all were right handed, and their ages ranged from 21 to 28. All subjects were considered fully trained because they all participated in an earlier pilot of the experiment. The experiment was approved by the Stanford University Institutional Review Board, and subjects gave informed consent.

3.3.2 Rigidity (Stiffness) Perception

Each subject sat in a chair facing the apparatus, as pictured in Figure 4. The setup consisted of the two unsupported, 1.5-inch cell devices placed side by side. Each device was rigidly attached to the top of a force/torque sensor in order to record the forces and torques applied over the course of the experiment. Both devices were surrounded by a curtained box so that subjects could touch the devices without visual feedback.

The two-alternative forced-choice experiment followed the method of constant stimuli [6]. Subjects were asked to freely explore the lumps on both devices and state which lump felt more

Figure 4: A subject interacts with the experimental apparatus. Two single-cell devices were placed side by side and covered by a curtain. Subjects were asked to state which device presented a larger stimulus (either rigidity or size) based on touch alone.

rigid. Both devices maintained a baseline chamber pressure of 0.6 psi in order to restore shape after every trial.

In each trial, one device presented a reference stimulus value, while the other presented a comparison stimulus value. The reference value was selected to be the middle of possible stiffness values based on the mechanical characterization results described in Section 4. A total of nine comparison values were selected so that four comparison values were smaller than the reference, four were larger than the reference, and one was equal to the reference. The extremes of the comparison values were selected to be the smallest and largest possible stiffnesses based on the experiments described in Section 3.2, and comparison values were equally spaced apart from the reference value.

Each of the nine comparison values was presented ten times in random order over the course of the experiment, and each comparison value was presented an equal number of times on each device to avoid a bias for one device over the other. Subjects were therefore asked to make a total of 90 stiffness comparisons. Subjects used the dominant hand to explore the devices until a decision was made; they recorded their responses by clicking either 'Left' or 'Right,' corresponding to which device they thought felt more rigid, on a computer GUI. Subject responses and force/torque data were recorded after every trial. There was no time limit for each trial, and subjects were asked to make their best guess if the decision seemed too difficult. Subjects were given an optional ten-minute break after after every forty-five trials.

3.3.3 Geometry Perception

After completing the stiffness perception trials, subjects performed trials related to perception of geometry (size of the ellipsoidal surface). They were asked to determine which of the two devices felt larger, following the same procedures described in Section 3.3.2. A total of nine geometry values were selected so that four comparison values were smaller than the reference, four were larger than the reference, and one was equal to the reference (see Section 4 for comparison values). The reference geometry value was selected to be the mean of the geometry values corresponding to 0.2 psi and 1.5 psi (the range of values tested in the data acquired in Section 3.2). This pressure range was chosen to correspond most closely to the curve fit in Figure 6 and to protect the air chamber from damage caused by too high of a pressure.

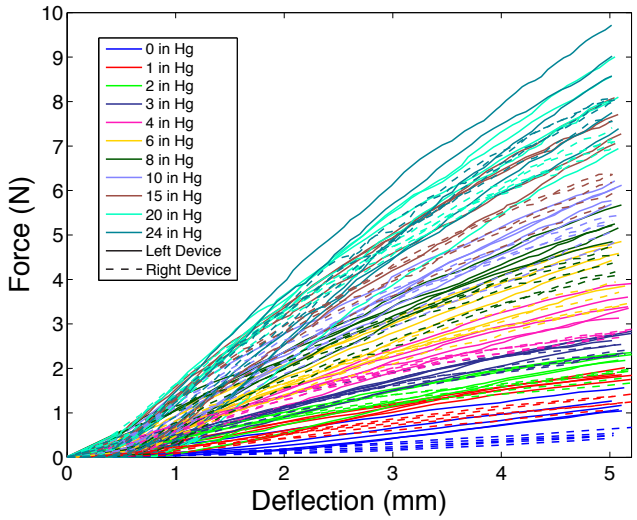

Figure 5: Force (N) plotted against deflection (mm) for all vacuum levels and both devices. The solid lines represent data from the device used on the left during the psychophysical experiments; the dashed lines represent data from the righthand device.

4 Results

4.1 Device Properties

The force-deflection data obtained from both devices were plotted together for all vacuum levels (Figure 5). We identified a deflection of 5 mm as a location where all the trials remained in the linear region. Based on research suggesting that stiffness is perceived as the force applied divided by the perceived penetration [18], we divided the force at 5 mm of deflection by 5 mm to obtain the stiffness. The average stiffness for each vacuum level was plotted against vacuum level (Figure 6).

The data obtained from the stiffness and shape data collection experiments described in Section 3.2 were found to satisfactorily follow the proposed model function shapes. For the relationship between rigidity and vacuum level, the fit had an R^2 value of 0.9904, and the parameters α_1, β_1, and γ_1 from Equation (1) were 121.0305 N/m, 215.0339 N/m, and 0.6269, respectively. For the relationship between 1/Eccentricity and chamber pressure, the fit had an R^2 value of 0.9908, and the parameters α_2 and β_2 from Equation (2) were 0.6965 and 0.4837, respectively.

Reference and comparison values for the psychophysical experiments were selected based on the curve fits. For stiffness, the reference value was chosen to be 929.9 N/m, the value halfway between the highest and lowest possible stiffnesses. The reference value was included as one comparison value, and the other comparison values were then chosen to be equally spaced apart (in stiffness values) from the reference value to the extremes on either side. The comparison values used in the stiffness psychophysical experiment were 121.0, 323.3, 525.5, 727.7, 929.9, 1132.1, 1134.3, 1536.6, and 1738.8 N/m.

For 1/Eccentricity, the reference value was chosen to be 0.584, the mean value of the eccentricities corresponding to 0.2 and 1.5 psi. The reference value was included as one comparison value, and the other comparison values were then chosen to be equally spaced apart (in *b/a* values) from the reference value to these boundary eccentricities. The comparison values used in the geometry psychophysical experiment were 0.320, 0.386, 0.452, 0.518, 0.584, 0.650, 0.716, 0.782, and 0.848.

4.2 Psychophysical Results

For the stiffness and size psychophysical experiments, the proportion of times each subject responded that the comparison value was

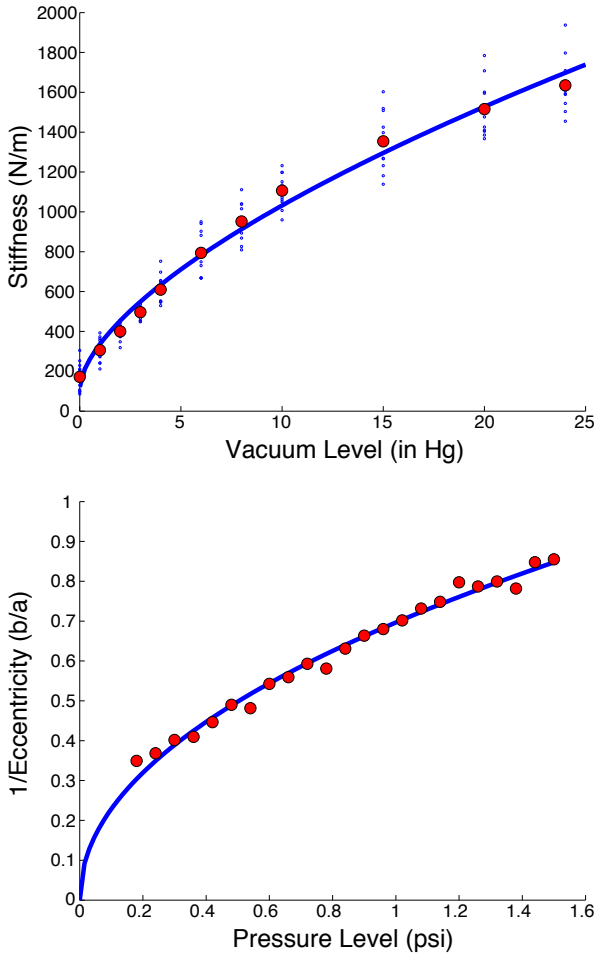

Figure 6: (Top) Stiffness (N/m) plotted against vacuum level (in Hg). Blue dots represent individual palpation trials, the red markers represent the average for all trials from each vacuum level, and the blue line is the power function curve fit. The R^2 value for the fit was 0.9904. All trials for both devices were plotted together due to high variability for each trial. (Bottom) 1/Eccentricity of a cell inflation profile plotted against chamber pressure (psi). The red markers represent data from an individual trial, and the blue line is the power function curve fit. The R^2 value for the fit was 0.9908.

greater than the reference value was plotted against the comparison values. A psychometric function was fit to each plot using the psignifit MATLAB toolbox (http://bootstrap-software.org/psignifit/). Example plots and fits for a representative subject are shown in Figure 7. The toolbox reports three relevant values: the PSE, the stimulus value corresponding to a proportion of 0.25 (J_{25}), and the stimulus value corresponding to a proportion of 0.75 (J_{75}). The JND is defined to be the mean of the differences between the PSE and these two J values, or

$$JND = \frac{(PSE - J_{25}) + (J_{75} - PSE)}{2} \tag{3}$$

The WF is calculated using

$$WF = \frac{JND}{PSE} \tag{4}$$

The results of the psychophysical experiments are summarized in Table 1. The average WF for stiffness perception was 16.0% with a standard deviation of 7.4%, and the average WF for size perception was 14.3% with a standard deviation of 2.6%. For each subject, the average peak force applied in the direction normal to the

Table 1: Results from the stiffness (left) and size (right) psychophysical experiments. For the stiffness experiment, mean peak force applied normal to the device surface (i.e. pressing down) was reported for each subject. For the size experiment, mean peak resultant torque in the plane of the device surface (i.e. pressing from side-to-side to determine shape) was reported for each subject..

	Rigidity (Stiffness) Perception Experiment				Geometry (1/Eccentricity) Perception Experiment			
Subject	JND (N/m)	PSE (N/m)	Weber Fraction (%)	Mean Peak z-Force (N)	JND (m/m)	PSE (m/m)	Weber Fraction (%)	Mean Peak xy-Torque (N*m)
1	231.5	1015.9	22.8	7.21	0.10	0.59	16.9	0.22
2	141.6	955.9	14.8	8.40	0.06	0.59	10.5	0.13
3	100.3	945.2	10.6	12.98	0.08	0.59	13.3	0.21
4	200.1	984.1	20.3	5.61	0.09	0.59	14.7	0.14
5	90.5	992.9	9.1	7.83	0.08	0.61	12.9	0.11
6	327.2	1263.2	25.9	5.44	0.11	0.60	18.5	0.14
7	183.2	858.4	21.4	8.17	0.08	0.59	13.4	0.08
8	162.8	998.8	16.3	10.59	0.07	0.59	12.1	0.10
9	28.0	908.5	3.0	8.97	0.10	0.59	16.4	0.12
Mean	162.74	991.42	16.03	8.36	0.09	0.59	14.33	0.14
Std. Dev.	87.63	113.22	7.40	2.36	0.02	0.01	2.61	0.05

plane of the device surface was calculated for each stiffness trial, and the average peak resultant torque in the plane of the device surface was found for each shape trial in order to test for correlations between any psychophysical metric (JND, PSE, or WF) and the forces/torques applied to the devices. After linear regression, minimal correlation ($R^2 \leq 0.4$) was found for all of these comparisons.

5 Discussion

When compared to WF values reported in other literature (as mentioned in the Section 2), the values found in our experiments seem reasonable for both stiffness and size. Additionally, no large correlation was found between forces/torques applied and subject perception (as described in the previous section), indicating that the subjects likely did not rely on applied forces to judge rigidity and size. This result seems promising for accurate portrayal of desired stiffnesses and geometries in future implementation of a medical training device, as the device may be used by people who apply different magnitudes of forces. The psychophysical metrics calculated in this paper can help optimize the designs of jamming systems for use as haptic displays. The JND and WF contribute insight into the ranges of stiffnesses and geometries that a device should be capable of outputting in order for the user to perceive a variety of tactile sensations from different configurations. They also help approximate the actuator resolution necessary for the device to display these ranges smoothly, as perceived by the human sense of touch.

Further psychophysical experiments could yield more information about human perception of these devices. The mean peak forces exerted by the subjects exceeded the maximum forces shown in Figure 5 because the subjects plastically deformed the devices during each trial. The experiments shown in Figure 5 served to characterize linear stiffness and so did not broach into the plastic regime. Additionally, the properties of the granular material may in fact change after repeated deformation. Future work can attempt to characterize the effects of repeated and plastic deformation on perception.

We also conducted these experiments using one baseline pressure for stiffness and no vacuum for geometry. These two properties, however, likely depend on each other, and so human perception of these two properties will also depend on each other. In addition, although the WF ideally remains constant for all reference values, this ideal needs to be tested and supported by experimental data.

Modifications to the devices used in the psychophysical experiments presented in this paper could yield more accurate results. During manufacturing, we realized that creating two completely identical devices was extremely difficult. The amount that a cell stiffens when subjected to vacuum or balloons when subjected to pressure depends the amount of coffee grounds within the cell, and despite use of a measuring spoon, the granular nature of the coffee grounds made it hard to tell exactly what volume of coffee grounds had been inserted into the cells. Additionally, the coffee grounds have a tendency to move within the cell, meaning that multiple palpations could present different stiffnesses (as shown by the high variability in the calculated stiffness values in Figure 6. Subject chose the left device more often than the right device (69.6% of the time, on average) in the size experiments, meaning that the amount of coffee grounds in each cell could have differed by a significant amount or that the compliance of the silicone could have differed. More systematic methods of mixing silicone and inserting coffee grounds may improve system performance and lower the JNDs.

6 Conclusion

Creating an effective tactile display and controlling it for haptic interactions requires sufficient understanding of the human perception of the physical properties it presents. We conducted a set of perceptual experiments to evaluate how the levels of vacuum and air pressure applied to our device affect the perception of size and rigidity in this particular setup. Quantitative measures of device output (stiffness and eccentricity) provided the basis for the reference levels and step sizes in each of the perceptual experiments. Data from all subjects fit sufficiently to psychometric functions and the mean JNDs, PSEs, and Weber fractions for both experiments are within range of similar metrics calculated for human perception of stiffness and size in prior research using other devices. This result suggests that our device is an effective means to present users with environments of varying stiffness and shape.

More thorough characterization of human perception of a Haptic Jamming display can be performed. In particular, we are interested in gauging the feasibility of using the device in medical simulation as a training tool for palpation tasks or other procedures that require a clinician to rely upon his or her sense of touch to make a diagnosis. For example, a Haptic Jamming display could alter its state to represent a variety of tissue types with embedded lumps of varying compliance to simulate tumors or fluid-filled cysts. Toward this end, we plan on conducting an exploratory palpation experiment to evaluate the effects of vacuum level, air chamber pressure, cell diameter, and thickness of a separate covering material on a user's ability to pinpoint the locations of lumps on a larger display.

Additionally, we plan on integrating a Haptic Jamming display onto the end effector of a robot that will move it around a larger workspace. The user will look at a spatially aligned virtual environment and freely explore the encountered-type haptic display beneath it. A hand tracker will allow the robot to move the display

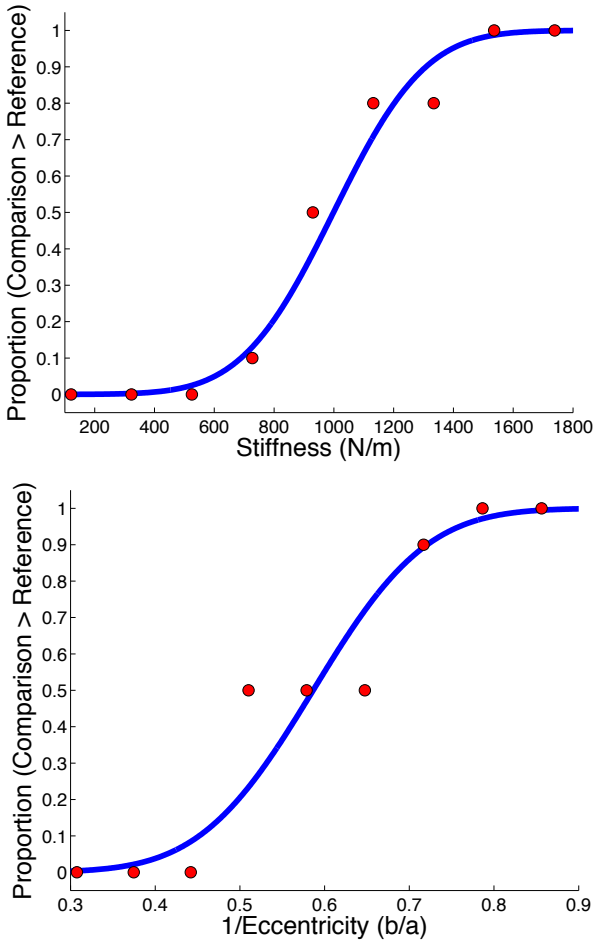

Figure 7: Example psychophysical data and psychometric function fits for a representative subject, Subject 8. (Top) The subject showed good discrimination of stiffness. Every value greater than the reference was judged to be greater, and every value lesser than the reference judged to be lesser, most of the time. (Bottom) The subject was not as discriminatory for size but was still able to locate values above and below reference most of the time..

to the current location of exploration and adjust the properties of the haptic jamming device to match the characteristics of that particular region of the environment. Further studies will examine the effects of adding this form of encountered-type haptic feedback on the realism of the virtual environment as a whole.

Acknowledgements

This work was supported by U.S. Army Medical Research and Materiel Command grant #W81XWH-11-C-0050 (to AMO), the National Science Foundation Graduate Research Fellowship Program (to AAS), and Stanford University (to AMG). Any opinions, findings, and conclusions or recommendations in this material are those of the authors and do not necessarily reflect the views of the sponsors.

References

[1] C. Wagner, S. Lederman, and R. Howe. A tactile shape display using RC servomotors. In *Symposium on Haptic Interfaces for Virtual Environment and Teleoperator Systems*, pp. 354-355, 2002.

[2] P. Taylor, D. Pollet, A. Hosseini-Sianaki, and C. Varley. Advances in an electrorheological fluid based tactile array. *Displays*, 18(3):135-141, 1998.

[3] Y. Liu, R. Davidson, P. Taylor, J. Ngu, and J. Zarraga. Single cell magnetorheological fluid based tactile display. *Displays*, 26(1):29-35, 2005.

[4] H. Zhu and W. J. Book. Control Concepts For Digital Clay. In *Proc. 7th IFAC Symposium on Robot Control*, pages 347-352, 2003.

[5] A. Stanley, J. Gwilliam, and A. Okamura. Haptic jamming: A deformable geometry, variable stiffness tactile display using pneumatics and particle jamming. In *Proc. IEEE World Haptics Conference*, pp. 25-30, 2013.

[6] G. Gescheider. *Psychophysics: Method, Theory, and Application*. 2nd ed., pp. 1-46. Hillsdale, New Jersey: Lawrence Erlbaum Associates, Inc, 1985.

[7] R. H. LaMotte. Softness discrimination with a tool. *Journal of Neurophysiology*, 83(4):1777-1786, 2000.

[8] P. E. Roland and H. Ladegaard-Pedersen. A quantitative analysis of sensations of tensions and of kinaesthesia in man. *Brain*, 100(4):671-692, 1977.

[9] M. A. Srinivasan and R. H. LaMotte. Tactual discrimination of softnesss. *Journal of Neurophysiology*, 73(1):88-101, 1995.

[10] H. Z. Tan, X. D. Pang, and N. I. Durlach. Manual resolution of length, force, and compliance. *In the Proceedings of the First Symposium on Haptic Interfaces for Virtual Environment and Teleoperator Systems, American Society of Mechanical Engineers Dynamic Systems and Control Division*, pp. 13-18, 1992.

[11] J. R. Amend, E. Brown, N. Rodenberg, H. M. Jaeger, and H. Lipson. A Positive Pressure Universal Gripper Based on the Jamming of Granular Material. *IEEE Transactions on Robotics*, Vol. 28, No. 2, pp. 341-350, 2012.

[12] N. G. Cheng, M. B. Lobovsky, S. J. Keating, A. M. Setapen, K. I. Gero, A. E. Hosoi, and K. D. Iagnemma. Design and analysis of a robust, low-cost, highly articulated manipulator enabled by jamming of granular media. In *Proc. IEEE International Conference on Robotics and Automation*, pp. 4328-4333, 2012.

[13] E. Steltz, A. Mozeika, N. Rodenberg, E. Brown, and H. M. Jaeger. JSEL: Jamming Skin Enabled Locomotion. In *Proc. IEEE/RSJ International Conference on Intelligent Robots and Systems*, pp. 5672-5677, 2009.

[14] S. Follmer, D. Leithinger, A. Olwal, N. Cheng, and H. Ishii. Jamming user interfaces: Programmable particle stiffness and sensing for malleable and shape-changing devices. In *Proc. ACM Symposium on User interface software and technology*, pp. 519-528, 2012.

[15] A. Mazzone, C. Spagno, and A. Kunz. The HoverMesh: A Deformable Structure Based on Vacuum Cells. In *Proc. ACM SIGCHI International Conference on Advances in Computer Entertainment Technology*, pp. 187-193, 2004.

[16] N. Aihara, T. Sato, and H. Koike. Highly deformable interactive 3D surface display. In *Proc. ACM Symposium on User Interface Software and Technology*, pp. 91-92, 2012.

[17] T. Mitsuda, S. Kuge, M. Wakabayashi, and S. Kawamura. Wearable force display using a particle mechanical constraint. *Presence: Teleoperators and Virtual Environments*, 11(6):569-577, 2002.

[18] A. Pressman, L. J. Welty, A. Karniel, and F. A. Mussa-Ivaldi. Perception of Delayed Stiffness. *The International Journal of Robotics Research*, 26(11-12), 1191-1203, 2007.